

50 MHz Reduced Noise Active Bandpass Filter using Current Feedback Amplifiers

K. A. Mezher^{#1}, N. T. Ali^{#2} & P. Bowron^{*3}

[#] Khalifa University of Science Technology and Research,

P.O. Box 573, Sharjah, United Arab Emirates

¹ kamezher@kustar.ac.ae

² ntali@kustar.ac.ae

^{*} School of Engineering, University of Bradford

Bradford, West Yorks., BD7 1DP, UK

³ p.bowron@brad.ac.uk

Abstract— In determining the dynamic range of analogue systems, the lower limit is defined by the rms output noise level V_{no} . A 50 MHz active bandpass filter (BPF) is designed and simulated using current feedback amplifiers (CFA). The designed circuit produced much lower noise level as well as better output signal level compared to traditional active BPF topologies. This is verified by signal and noise spectral-analysis simulation, which is compared with well known active-RC filter circuits.

I. INTRODUCTION

In the last few years there was an increasing interest in active filters using CFA although they were available over 2 decades ago [1-5]. They offer wide bandwidth and excellent video characteristics [6]. However, the disadvantages of these devices are the restriction to certain active filter topologies and restricted feedback resistor values due to stability issue [7]. Also, it was reported that filters using these devices produce lower dynamic range as compared to the common voltage operational amplifiers [8].

II. BANDPASS FILTER DESIGN

The versatility of the operational amplifier has led to a multitude of different circuit configurations to realize 2nd-order filters that uses single or multiple devices. However, single-amplifier circuits are of particular interest due to their obvious advantages of low power consumption, low component count, low cost and absolute stability that are well documented in the literature. Well known Sallen-Key circuits [9] are selected and designed to achieve the optimum performance possible in terms of signal and noise levels.

Figure 1 shows a positive feedback controlled-gain single amplifier BPF. The circuit is designed for unity gain (0 dB) and Q and 50MHz centre frequency. The frequency deviation due to parasitic effect is taken into consideration and included in the practical capacitor selection. The RF simulated (using MULTISIM 9 RF simulation tool) signal performance is shown in figure 2. It shows that the actual achieved gain is -4.93dB at 43.19 MHz, which is much less than the designed 0dB gain and 50 MHz centre frequency.

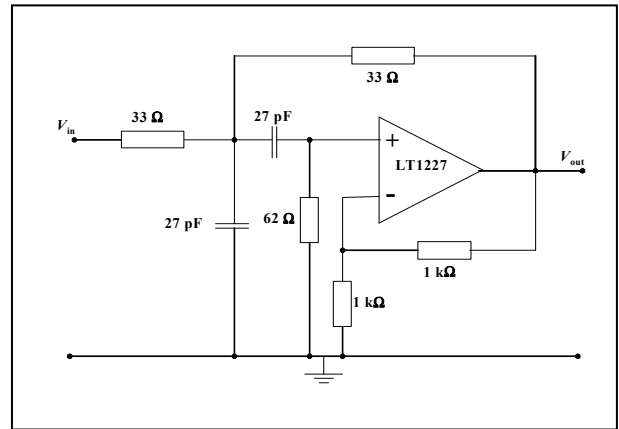


Fig. 1: Sallen-Key positive feedback controlled-gain single amplifier BPF (with $K_o=1$, $Q=1$ and $f_o=50\text{MHz}$).

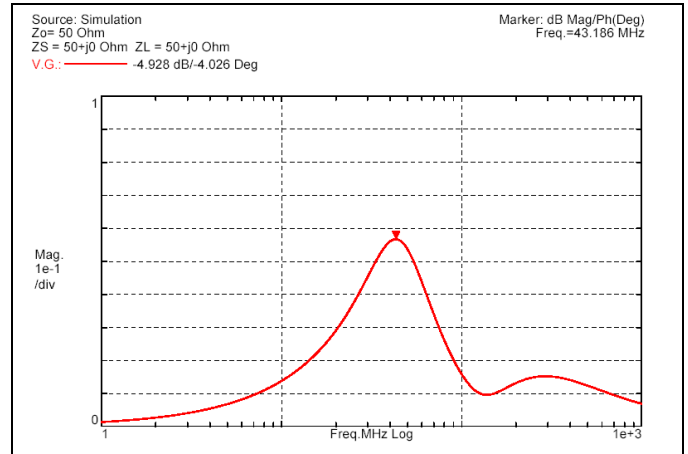


Fig. 2: RF simulated output signal frequency response for single amplifier BPF circuit of Fig. 1.

Figure 3 shows a second circuit that cascades Sallen-Key positive feedback single amplifier 2nd-order lowpass and high pass filters to achieve a bandpass frequency response. The circuit is also designed for unity gain (0 dB) and Q and

50MHz centre frequency. The RF simulated signal performance is shown in figure 4. It shows that the actual achieved gain is -1.1dB at 49.6 MHz, which is much better than the previous circuit.

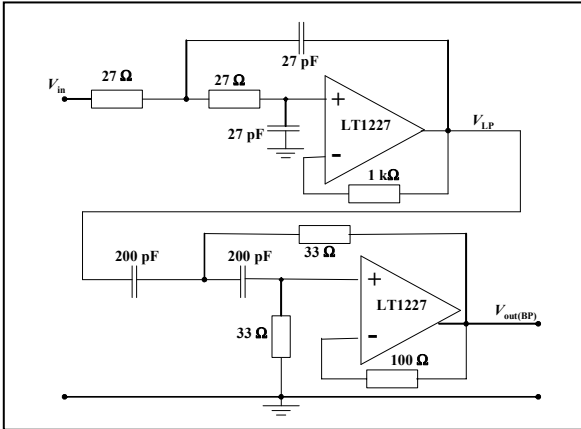


Fig. 3: Cascaded BPF circuit (with $K_o=1$, $Q=1$ and $f_o=50\text{MHz}$).

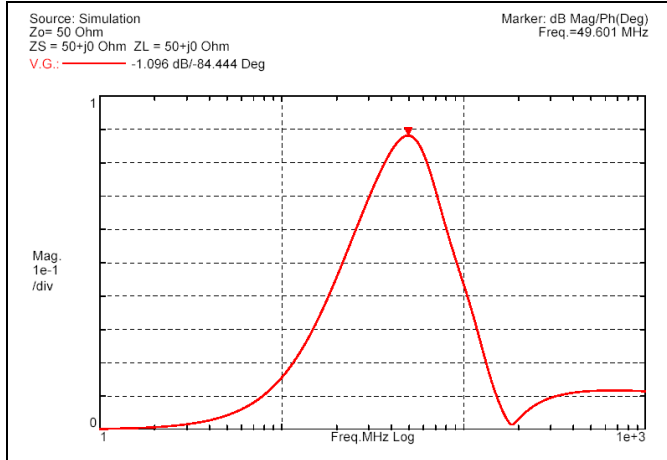


Fig. 4: RF simulated output signal frequency response for cascaded BPF circuit of Fig. 3.

Similar performance is achieved for both circuits using the S21 (Transducer power gain) simulation tool, although at lower frequency than V.G. for the cascaded circuit, as shown in figures 5 and 6.

III. NOISE ANALYSIS AND SIMULATION

By superposition, the general noise block diagram for an active network comprising M amplifiers gives [10] the total squared noise voltage spectral density at the output of the l'th amplifier as

$$E_{no_l}^2 = \sum_{m=1}^M |T_{no_{lm}}|^2 E_{nm}^2 \quad (1)$$

Here, E_{nm}^2 is the overall equivalent squared noise voltage spectral density at the input of the m'th amplifier, which includes all active and passive noise contributions. However, the active input noise current density source must now be considered due to its large value in CFA ($E_{na} = 3.2 \text{ nV}/\sqrt{\text{Hz}}$ and inverting $I_{na} = 32 \text{ pA}/\sqrt{\text{Hz}}$ [5]). The noise current source was neglected with voltage operational amplifiers due to its small value as compared to noise voltage spectral density [9]. Eqn. (1) omits the source noise, which will be significant if driven from the output of another network and must be taken into account with the combined input noise source.

At angular frequency ω ,

$$T_{no_{lm}}(j\omega) = \frac{E_{no_l}(j\omega)}{E_{nm}} \Big|_{E_{nl}=0, (l \neq m)}. \quad (2)$$

is the noise transfer function from the input of the m'th amplifier to the output of the l'th amplifier (in the absence of all other noise sources).

Following Eqn. (1), for all second-order networks, the squared output noise spectral density is in the form

$$E_{no}^2(\omega) = E_{LP}^2 |T_{LP}(j\omega)|^2 + E_{BP}^2 |T_{BP}(j\omega)|^2 + E_{HP}^2 |T_{HP}(j\omega)|^2 \quad (3)$$

$T_{LP}(j\omega)$, $T_{BP}(j\omega)$ are the normalised lowpass and bandpass transfer functions, respectively, being given for a second-order circuit [11] by

$$T_{LP}(j\omega) = \frac{\omega_o^2}{(\omega_o^2 - \omega^2) + j\omega \frac{\omega_o}{Q}} \quad (4a)$$

and

$$T_{BP}(j\omega) = \frac{j\omega\omega_o^2}{(\omega_o^2 - \omega^2) + j\omega \frac{\omega_o}{Q}} \quad (4b)$$

Since the corresponding highpass function is

$$|T_{HP}(j\omega)|^2 = (2 - \frac{1}{Q^2}) |T_{BP}(j\omega)|^2 - |T_{LP}(j\omega)|^2 + 1 \quad (5)$$

then

$$E_{no}^2(\omega) = E_{n\alpha}^2 |T_{LP}(j\omega)|^2 + E_{n\beta}^2 |T_{BP}(j\omega)|^2 \quad (6)$$

where $E_{n\alpha}$ and $E_{n\beta}$ are frequency-independent variables obtained by combining related LP and BP noise terms.

The total rms output noise voltage V_{no} is given [12] by integrating the spectral density over a prescribed angular-frequency band ω_1 to ω_2 :

$$V_{no}^2 = \frac{1}{2\pi} \int_{\omega_1}^{\omega_2} E_{no}^2(\omega) d\omega \cong \frac{1}{2\pi} \int_0^{\infty} E_{no}^2(\omega) d\omega \quad (7)$$

Substituting Eqns. (4a) & (4b) in Eqn. (6) and applying the known [11], [12] properties:

$$\int_0^{\infty} |T_{LP}(j\omega)|^2 d\omega \equiv \int_0^{\infty} |T_{BP}(j\omega)|^2 d\omega = \frac{\pi}{2} \omega_o Q \quad (8)$$

then Eqn. (7) gives

$$V_{no}^2 = \frac{\omega_o Q}{4} (E_{n\alpha}^2 + E_{n\beta}^2) \quad (9)$$

From Eqns. (4a) & (4b), at the centre frequency (i.e. $\omega = \omega_o$),

$$|T_{LP}(j\omega)|^2 = |T_{BP}(j\omega)|^2 = Q^2 \quad (10)$$

which substituted into Eqn. (6) gives

$$(E_{n\alpha}^2 + E_{n\beta}^2) = \frac{E_{no}^2(\omega_o)}{Q^2} \quad (11)$$

Then, substituting into Eqn. (9),

$$V_{no}^2 = \frac{1}{4Q^2} (\omega_o Q) E_{no}^2(\omega_o) \quad (12)$$

where $E_{no}(\omega_o)$ is the measured output spectral density at the centre frequency. Q 's are not cancelled in order to preserve the universal ($\omega_o Q$) factor. Eqn. (12) enables measurements of noise spectral density to be converted into rms output noise voltage that then directly used in the well known dynamic range equation [9].

The simulated noise spectrum (using Multisim 9 RF simulator) for both single-amplifier and cascaded bandpass filter circuits are shown in figures 7 and 8 respectively. It shows that the noise spectral density at centre frequency $E_{no}(\omega_o)$ for the circuit of Fig. 1 is 53.2 nV/Hz as compared to 39.3 nV/Hz for the circuit of Fig. 2. This represents a 26% noise reduction in the 2nd circuit.

IV. CONCLUSIONS

It is demonstrated that the output noise level of 2nd-order active filter can be completely defined on a theoretical basis at such high frequencies. The succinct relation in Eqn. (12) is particularly useful for determining rms output voltage from the measured spectral density for any 2nd-order active-RC filter circuit. In conjunction with the large-signal limit, the dynamic range of the circuit can be directly evaluated.

Simulation results shows that cascaded 2nd-order active filter sections produces improved output signal level and much lower output noise voltage spectral density. For our particular design, it produced 26% noise reduction as compared to single amplifier filter structure for similar design specifications.

The above results have implications on the dynamic range performance of active filters operating at these frequency ranges.

REFERENCES

- [1] S. N. Ahmad, "Realisation of high input impedance universal filter using current-feedback amplifiers", J. of Active and Passive Electronic Devices, vol. 1, pp. 137-143, 2005.
- [2] M. T. Abuelma'atti & H. A. Al-Zaher, "New grounded-capacitor grounded-resistor controlled universal filter using current-feedback amplifiers", Proc. Nati. Sci. Counc. ROC(A), vol. 24, No. 3, pp. 205-209, 2000.
- [3] J. W. Horng & M. H. Lee, "High input impedance voltage-mode lowpass and highpass filter using current-feedback amplifiers", Electronics Letters, vol. 33, pp. 947-948, 1997.
- [4] Fairchild Semiconductor Corporation, "Designing with current feedback amplifiers", 2006.
- [5] C. Sanchez-Lopez, E. Tlelo-Cuautle, M. Fakhfakh and M. Loulou, "Computing simplified noise-symbolic-expressions in CMOS CCs by applying SPA and SAG", IEEE ICM 2007, pp. 159-162, Cairo, Egypt, 2007.
- [6] Linear Technology Corporation, "LT1227 current feedback amplifier application note", Datasheet, 1994.
- [7] B. Carter, "A current feedback op-amp circuit collection", Texas Instruments Application report, 2001.
- [8] P. Bowron, K. A. Mezher & H. W. Ng, "A performance assessment of audio filters using current-mode analogue devices", IEE Colloquium on Digital and Analogue Filters and Filtering Systems, pp. 15/1-15/4, London, UK, 30 Nov. 1995.
- [9] J. Karki, "Analysis of the Sallen-Key architecture", Texas Instruments Application report, 2002.
- [10] P. Bowron and K. A. Mezher, "Noise analysis of second-order analogue active filters", IEE Proc. Circuits Devices Syst., vol. 141, pp. 350-356, 1994.
- [11] H.J. Bächler & W. Guggenbühl, "Noise analysis and comparison of second-order networks containing a single amplifier", IEEE Trans. Circuits & Systems, vol. 27, pp. 85-91, 1980.
- [12] F.N. Trofimenkoff, D.H. Treleaven and L.T. Bruton, "Noise performance of RC-active quadratic filter sections", IEEE Trans. Circ. Theory, vol. 20, pp. 524-532, 1973.

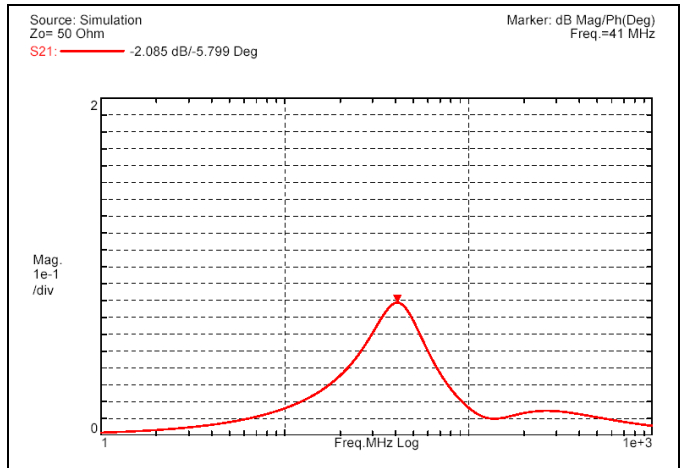


Fig. 5: Simulated S21 parameter for single amplifier BPF circuit of Fig. 1.

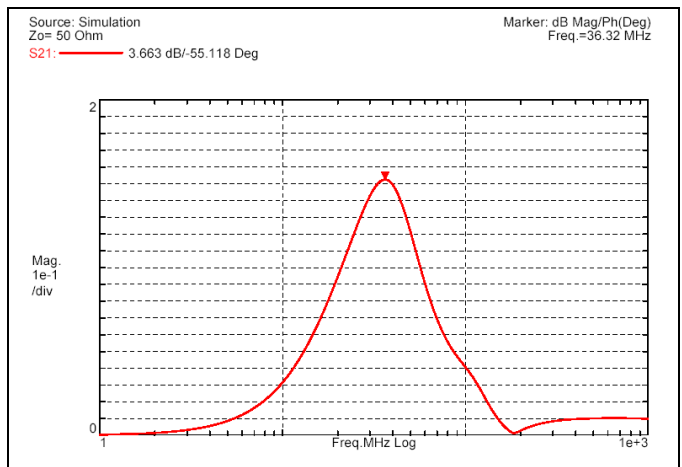


Fig. 6: Simulated S21 parameter for cascaded amplifier BPF circuit of Fig. 3.

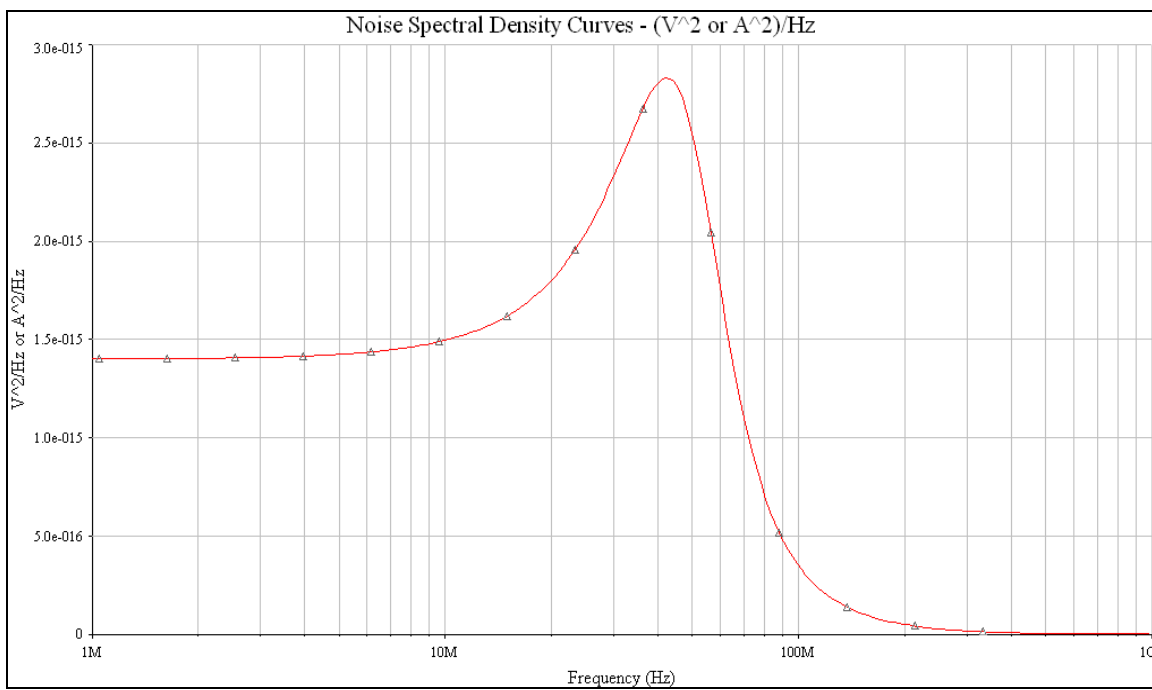


Fig. 7: Simulated noise spectral density for circuit of Fig. 1.

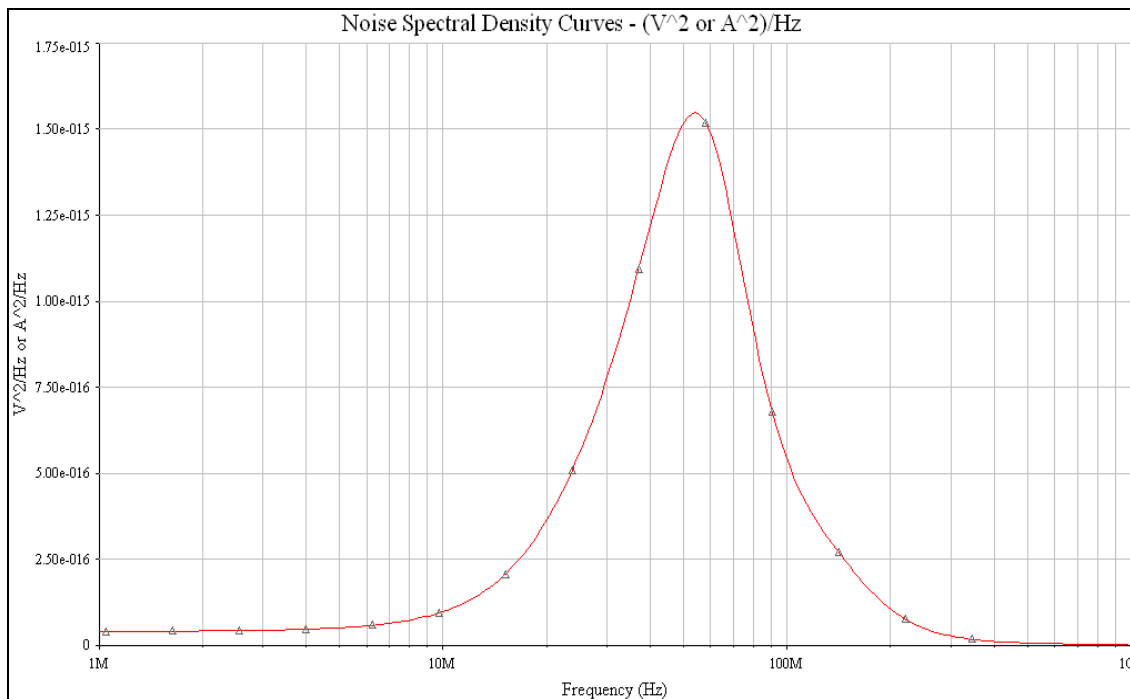


Fig. 8: Simulated noise spectral density for circuit of Fig. 3.